OSIPI Open Science Initiative for Perfusion Imaging

OSIPI Task Force 4.1:

Arterial Spin Labeling perfusion imaging and analysis lexicon and reporting recommendations (v0.1)

Task Force 4.1 leads:

Lead: David Thomas	UCL Queen Square Institute of Neurology, London, UK
Co-Lead: Yuriko Suzuki	Wellcome Centre for Integrative Neuroimaging, FMRIB University of Oxford, UK

Task force 4.1 members (alphabetical order):

Patricia Clement	Department of Diagnostic Sciences, Ghent University, Belgium
Weiying Dai	State University of New York at Binghamton, USA
Sudipto Dolui	University of Pennsylvania, USA
María Fernández Seara	Clinica Universidad de Navarra, Spain
Thomas Lindner	University Hospital Hamburg-Eppendorf, Germany
Henk-Jan Mutsaerts	Amsterdam UMC, Netherlands
Jan Petr	Helmholtz-Zentrum Dresden-Rossendorf, Dresden, Germany
Xingfeng Shao	University of Southern California, USA
Manuel Taso	Beth Israel Deaconess Medical Center, USA

ISMRM ONE COMMUNITY FOR CLINICIANS AND SCIENTISTS

OSIPI Open Science Initiative for Perfusion Imaging

External contributors

Expert panel (alphabetical order)

Michael Chappell	Sir Peter Mansfield Imaging Centre, School of Medicine, University of Nottingham, UK
Luis Hernandez-Garcia	FMRI Laboratory, University of Michigan, USA
Jia Guo	Department of Bioengineering, University of California Riverside, USA
Thomas Okell	Wellcome Centre for Integrative Neuroimaging, FMRIB University of Oxford, UK
Qin Qin	The Russell H. Morgan Department of Radiology and Radiological Science, Johns Hopkins University, USA
Eric Wong	CFMRI, Department of Radiology, University of California San Diego, USA
Joseph Woods	Wellcome Centre for Integrative Neuroimaging, FMRIB University of Oxford, UK

Manufacturers (alphabetical order)

Suchandrima Banerjee	GE Healthcare
Josef Pfeuffer	Siemens Healthcare
Valentin Prevost	Canon Medical Systems Corporation
David Shin	GE Healthcare
Takashi Tsuneki	FUJIFILM Healthcare Corporation
Kim van de Ven	Philips Healthcare
Marta Vidoretta	Siemens Healthcare

ISMRM ONE COMMUNITY FOR CLINICIANS AND SCIENTISTS

OSIPI Open Science Initiative for Perfusion Imaging

Table of Contents

ISMRM ONE COMMUNITY FOR CLINICIANS AND SCIENTISTS

Introduction

Perfusion images can be obtained by using Arterial Spin Labeling (ASL), where nuclear spins in arterial blood water are labeled by radiofrequency (RF) pulses and gradients. The labeled blood acts as an endogenous tracer, allowing ASL to provide non-invasive perfusion imaging without the injection of an exogenous contrast agent. Following publication of the ASL consensus statement for the recommended implementation of ASL perfusion MRI for clinical application in the brain (Alsop et al., 2015) by the Perfusion Study Group of the International Society for Magnetic Resonance in Medicine (ISMRM) and the EU-COST 'ASL in Dementia' action in 2014, basic ASL perfusion imaging has now been implemented by the majority of MRI manufacturers. A standardized implementation, and the increased availability of ASL, has encouraged the use of ASL in clinical applications. Motivated by the non-invasive nature of ASL perfusion imaging, there is an increased number of cohort studies adopting ASL perfusion imaging, such as the Alzheimer's Disease Neuroimaging Initiative (ADNI3; http://adni.loni.usc.edu/adni-3/) and some branches of the Human Connectome Project (https://www.humanconnectome.org/study/structural-functional-connectome-across-ad-subtypes), in which data are acquired from multiple sites using different MRI scanners. To maximize the benefit of these data, guidelines for consistent reporting of image acquisition and analysis parameters is essential.

The development of new ASL techniques has continued to improve cerebral blood flow (CBF) quantification and provide functionalities additional to conventional CBF measurements. These advances have greatly expanded the scope of ASL, but also bring further divergence of the technique, which can hamper research reproducibility.

As part of the Open Science Initiative for Perfusion Imaging (OSIPI) (www.osipi.org/), the purpose of this document is to develop standardized nomenclature for the broad range of ASL imaging techniques and parameters, as well as the physiological constants required for quantitative analysis. We aim to achieve harmonization with other parallel efforts, such as the above-mentioned ASL consensus statement and the Brain Image Data Structure (BIDS) ASL extensions (please see the following subsection "Previous efforts on ASL standardization relevant to this document").

The resulting ASL lexicon is intended to form a common, community-endorsed recommendation for reporting of ASL perfusion imaging, detailing which and how parameters in acquisition protocols and analysis should be reported, aiming to improve the reproducibility of the reported studies. In the future, this lexicon could also be used to improve the Digital Imaging and Communications in Medicine (DICOM) standard for the purposes of communicating raw images and parametric maps of ASL perfusion MRI.

Previous efforts on ASL standardization relevant to this document

"Recommended Implementation of Arterial Spin-Labeled Perfusion MRI for Clinical Applications: A Consensus of the ISMRM Perfusion Study Group and the European Consortium for ASL in Dementia" (Alsop et al., 2015)

- A consensus paper of recommended implementations of ASL perfusion imaging for clinical applications, put together by an expert group of members of the Perfusion Study Group of the International Society for Magnetic Resonance in Medicine (ISMRM) and the European 'ASL in Dementia' consortium.

Brain Image Data Structure (BIDS) (Gorgolewski et al., 2016) ASL extensions

- A community effort to standardize how to organize and share neuroimaging datasets, which was extended to include ASL in 2021:
  - https://bids-specification.readthedocs.io/en/stable/04-modality-specific-files/01-magnetic-resonance-imaging-data.html#arterial-spin-labeling-perfusion-data
  - Preprint DOI 10.31234/osf.io/e87y3

"Consensus-based technical recommendations for clinical translation of renal ASL MRI" (Nery et al., 2020)

- Technical recommendations for renal ASL from an international group of experts working under the framework of the PARENCHIMA project, funded by a European Cooperation in Science and Technology (COST) Action.

Currently (October 2021), a series of updates to the 2015 ASL consensus paper, aka "ASL Grey Papers", are being written on the following topics (tentative titles):

- Recent technical development in ASL: A Review of the State of the Art
- Recommendations for perfusion MRI with multi-time point Arterial Spin Labeling
- Velocity Selective Arterial Spin Labeling Perfusion MRI: A Review of the State of the Art and Recommendations for Clinical Application
- Arterial Spin Labeling – A position statement on how to interpret Arterial Spin Labeled Perfusion Images in clinical neuroimaging applications
- Body ASL: an update on state-of-the-art for applications outside of the brain

Development of this document

The overall structure of this document was implemented by the OSIPI Task force 4.1 members from June 2020 to April 2021. The draft v0.1 was then sent out for consultation to experts of the field, as well as major MRI vendors, from May to July 2021. The experts of the field were chosen from the authors of the above mentioned "ASL Grey Papers". The names of the external contributors are listed here. Their feedback is integrated into the draft document, and the draft v0.2 is published in August 2021. The draft v0.2 is shared with the members of the ISMRM Perfusion Study Group and all members are invited to leave their comments/suggestions on the document using Google Doc until the end of October 2021. Also, a Slack channel is provided to allow discussions among the Perfusion SG members during that period.

Update of this document

The document will be continuously amended by perfusion researchers who wish to contribute.

Target audience

This document is primarily intended to provide:

- a guideline for developers of ASL sequences and analysis tools to conform to consensus recommendations, to avoid misunderstandings caused by diverse terminologies and inconsistent definitions.
- a lexicon for researchers to find how their ASL studies and results should be documented and reported, which should make their studies more understandable and reproducible.

This document is, however, not intended to provide recommendations for the choice of imaging techniques, sequence parameter values and analysis approaches, which can be found in the relevant literature (e.g. the ASL consensus paper). Although values for ASL sequence parameters and physiological constants are provided in this document, these are merely examples taken from the literature, and are *not* intended to be taken as recommendations for general use.

Organization of this document

This document is separated into two main parts: (i) ASL Lexicon and (ii) Reporting Recommendations.

The **ASL Lexicon** consists of several sections:

- Section 1: Generic Definitions in ASL
- Section 2: Labeling Methods
- Section 3: Parameters in ASL Labeling Module
- Section 4: Readout Module
- Section 5: Derivative Parameters in ASL
- Section 6: Physiological Parameters and Constants for Quantification

In the **Reporting Recommendations**, there are two lists of parameters that are categorized with two recommendation levels:

- Required: parameters that are essential for meaningful interpretation of the ASL data and for quantitative analysis. These must be included in an ASL publication in order for its data set to be 'OSIPI compliant'.
- Recommended: parameters that are useful for interpretation of the ASL data and could explain specific characteristics or systematic differences between data sets. We encourage authors to include as many of these as possible in ASL publications.

Importantly, the content of this document is not meant to be a complete list of all existing techniques, but rather a dynamically growing inventory that is intended to be extended by the community as further methods and improvements are developed.

Part 1: ASL Lexicon

The ASL Lexicon aims to organize comprehensive lists of terminology for ASL imaging techniques and acquisition parameters, as well as physiological constants and parameters required in quantitative analysis. The ASL Lexicon consists of seven sections, and within each individual section, methods/parameters are organized into tables, with the following items to be listed, if applicable:

- **Name:** A unique name for the parameter or methods.
- **Notation:** If applicable, a commonly used abbreviation.
- **Description:** A short definition or specification; if available, a mathematical formula will be utilized to provide a unique description of the quantity, regardless of varying nomenclature and interpretation.
- **Unit:** If applicable, the general physical units.
- **Reference:** key literature establishing the concept or corresponding analysis method and providing relevant details. If applicable, the publication first introducing the respective technique is cited. For general concepts and quantities, review papers will be cited which give an overview of the general concept.

In this document, the term "***labeling***" is used in the description throughout all techniques, which is however interchangeable with "***tagging***".

Section 1: Generic Definition in ASL

In this section, the basic structural elements of the standard ASL sequence are listed and defined. Detailed descriptions of the basic principles of ASL can be found in several excellent technical review articles and book chapters, e.g. (Alsop et al., 2015; Barker et al., 2013; Golay et al., 2004; Wong, 2005).

OSIPI Name	***Description***
Arterial Spin Labeling (ASL)	Any MRI technique in which contrast is generated by manipulation of the arterial blood magnetization using RF pulses prior to image acquisition, with the aim of isolating inflowing signal for flow/perfusion quantification.

Labeling pulse	RF pulse, or train of RF pulses, intended to change the magnetization state of blood in order to differentiate it from stationary tissue. In general, labeling pulses can be spatially selective, targeting the blood outside the imaging volume (upstream), or velocity/acceleration selective (VS/Acc), targeting blood without special selectivity (i.e. including blood flowing within the imaging volume) according to its velocity or acceleration.
Control pulse	RF pulse, or train of RF pulses, intended to match the static tissue Magnetization Transfer (MT), diffusion, eddy currents, or any other side effects of the labeling pulse, while causing minimal perturbation to arterial blood.
Labeled image	Image acquired after preparation by a labeling pulse.
Control image	Image acquired after preparation by a control pulse.
Delay time	The time interval between the end of labeling and the image readout that allows the labeled arterial blood bolus to reach the tissue of interest. In general, it is called the Post-Labeling Delay (PLD) in pseudo-continuous ASL (PCASL) and Inflow Time (TI) in Pulsed-ASL (PASL). In VSASL, both TI and PLD are used to define different temporal parameters. See the section "Parameters in ASL labeling module" and Figures section below for more details.
Single PLD/TI	ASL protocol in which images are acquired with a single delay time.
Multiple PLD/TI	ASL protocol in which images are acquired with multiple (more than one) delay times.
Background suppression (BS)	Strategy for reduction of static tissue signal intensity using a train of RF pulses applied prior to image readout. The aim of background suppression is to improve SNR of the ASL image by reducing signal fluctuations in the labeled and control images. There are many background suppression schemes available, involving saturation and inversion pulses.

Saturation	Saturation of the imaging volume is performed just before and/or after the labeling and control pulses, to set its longitudinal magnetization to zero and thereby eliminate any label/control MT or slice profile mismatches. Water suppression enhanced through T1 effects (WET) pulses (Ogg et al., 1994) with four pulses are commonly used (Golay et al., 2005).
Vascular suppression	Reduction of signal present in larger arterial vessels at the time of imaging. Generally, it is achieved by applying crusher gradients after the excitation pulse, which selectively dephases signal based on the velocity profile of the spins in the direction of the gradient (Petersen et al., 2006). In VSASL, vascular suppression is achieved using velocity selective saturation pulses.
M0 image (also known as proton density image)	Additional calibration image required for blood flow quantification, used to estimate the fully-relaxed magnetization (M0) of blood (M0b) and tissue (M0t), which are necessary to calculate perfusion from ASL images. M0 image is commonly obtained as a proton density image by turning off all preparation pulses before acquisition while using a relatively long TR. When background suppression pulses are not applied, the average (mean) control image can be used as the M0 image by correcting for T1 relaxation.

Section 2: ASL Labeling Methods

Subsection 1: (Pseudo-) Continuous ASL

Name	***Notation***	***Description***	***References***
Continuous ASL	**CASL**	A single, continuous-wave, RF pulse applied over a long period, typically 1-3s, in combination with a constant magnetic field gradient. Arterial blood is continuously inverted as it flows through a specified labeling plane by	(Alsop and Detre, 1998, 1996; Williams et al., 1992)

		means of flow-driven adiabatic inversion.	
Pseudo-continuous ASL	**PCASL**	Similar to CASL, labeling occurs over a long period, typically 1.5-2s and inverts flowing arterial blood. In PCASL, however, a train of short RF pulses applied at a rate of approximately one per millisecond replaces the single, continuous pulse of CASL. For the control scan, phase modulation of the RF pulse train is applied, such that magnetization transfer effects are identical to the labeling scan, but the arterial blood magnetization is unperturbed. Note that the mechanism of arterial blood inversion is equivalent for CASL and PCASL and, consequently, the quantification model is the same.	(Dai et al., 2008)
Balanced PCASL	**bPCASL**	PCASL implementation which uses the same gradient waveform for the label and control pulses.	
Unbalanced PCASL	**ubPCASL**	PCASL implementation which uses different gradient waveforms for the label and control pulses, so that the average gradient (G_{av}) becomes zero for the control. If optimized, improved robustness to off-resonance effects at the labeling plane can be achieved compared to bPCASL.	
Separate RF labeling coils		Using separate, dedicated RF transmission coils (i.e. in addition to the RF transmit coils for imaging) positioned over the artery/arteries of interest , to	(Mora Álvarez et al., 2019; Talagala et al., 2004;

		reduce power deposition and avoid MT effects in the perfused organ	Zhang et al., 1995)
Flow encoding arterial spin tagging	**FEAST**	A technique based on (P)CASL that acquires a pair of ASL subtraction images with and without crusher gradients for vascular suppression. The ATT is calculated using the ratio between (P)CASL images with and without vascular suppression	(Wang et al., 2003)

Subsection 2: Pulsed ASL

Name	***Notation***	***Description***	***References***
Pulsed ASL	**PASL**	A general term for ASL methods with a single (or limited number of) short RF pulse(s) (typically 10-20 ms) applied to 'instantaneously' invert a slab of arterial blood magnetization.	(Alsop et al., 2015)
Echo-Planar Imaging and Signal Targeting with Alternating Radiofrequency	**EPISTAR** **STAR** (non-EPI readout)	Version of PASL in which the label is performed by a slab-selective adiabatic inversion pulse applied proximal to the imaging volume/slices. In the original multi-slice implementation, the control preparation was achieved by applying slab-selective RF pulses over the same region as the label, with total power matched to the labeling inversion pulse (to generate the same MT effects across the imaging volume) but which result in minimal perturbation of the arterial blood magnetization e.g. two	(Edelman and Chen, 1998; Petersen and Golay, 2007)

		consecutive inversion pulses with half power. In the Philips product implementation, the control preparation is achieved by mirroring the RF amplitude and frequency modulation for the second part of the adiabatic pulse.	
Flow-Sensitive Alternating Inversion Recovery	**FAIR**	Version of PASL in which the label is performed by a non-slice-selective global inversion pulse, while the control image is obtained using a slice-selective inversion pulse applied to the imaging slab. Because of this symmetric nature, FAIR allows inflow of the labeled blood from both sides of the imaging volume.	(Kim, 1995)
Proximal Inversion with Control for Off-Resonance Effects	**PICORE**	Version of PASL, in which the label is the same as in EPISTAR, while the control image is obtained using an off-resonance inversion pulse that is applied with the same frequency offset as the label, but without a slab-selective gradient.	(Wong et al., 1997)
Double Inversions with Proximal Labeling of bOth tag and control iMAges	**DIPLOMA**	Version of PASL designed to reduce the residual MT mismatch between the label and control images observed in EPISTAR and PICORE. In both label and control, two consecutive adiabatic inversion pulses are applied; in the labeling preparation, application of an off-resonance inversion pulse (similar to the one applied in PICORE for control preparation) is followed by a slab-selective inversion pulse. In the	(Jahng et al., 2003)

		control preparation, two slab-selective inversion pulses are applied.	
Transfer insensitive labeling technique	**TILT**	Version of PASL, in which labeling is achieved by two successive 90° radiofrequency (RF) pulses. For the control, the phase of the second pulse is shifted by 180°, thereby yielding no net effect on blood water magnetization.	(Golay et al., 1999)
Bolus cut-off technique		In PASL, the bolus duration (see Section 3) of labeled blood is unknown a priori, and depends on the labeling slab thickness and blood flow velocity. To achieve accurate quantification of CBF with a single TI acquisition, several techniques have been proposed to define the bolus duration, as described below.	
Quantitative Imaging of Perfusion Using a Single Subtraction	**QUIPSS**	QUIPSS aims to eliminate arterial transit time effects in PASL, to enable reliable quantification of CBF with a single TI acquisition. This is achieved by applying a saturation RF pulse to the imaging volume at a time TI1 after labeling, where TI1 is greater than the arterial transit time, followed by image acquisition at time TI. N.B. this approach has not been widely adopted due to the prevalence of intravascular signal in the ASL difference images.	(Wong et al., 1998a)
Quantitative Imaging of Perfusion Using a Single Subtraction II	**QUIPSS-II**	QUIPSS-II aims to control the bolus duration in PASL and allow reliable quantification of CBF when using PASL with a single TI. This is achieved by applying a saturation RF slab to the area	(Wong et al., 1998a)

		where the labeling RF slab is applied, thereby cutting off the "tail" of the labeled bolus. See "Bolus duration" for the definition.	
QUIPPS II with thin-slice TI_1 periodic saturation	**Q2TIPS**	Modified version of QUIPSS-II, aiming to improve the saturation efficiency by replacing the QUIPSS-II saturation pulse with multiple thin RF saturation pulses applied at the distal edge of the labeling slab.	(Luh et al., 1999)
QUIPSS II with window-sliding saturation sequence	**Q2WISE**	A hybrid technique between Q2TIPS and QUIPSS II. In Q2WISE, saturation is achieved by using 2 thin saturation pulses and 1 thick slab saturation pulse to reduce the RF power deposition	(Song et al., 2012)
Wedge-shaped PASL	**WS-PASL**	Version of PASL, in which a wedge-shaped adiabatic inversion pulse is used to directly control the bolus duration in different vessels based on the flow velocity.	(Guo et al., 2016)
Attenuating the static signal in arterial spin tagging	**ASSIST**	FAIR ASL approach with multiple inversion pulses during the inflow time to suppress static tissue signal (first implementation of background suppression with ASL)	(Ye et al., 2000)

Subsection 3: Velocity-selective ASL

Name	***Notation***	***Description***	***References***
Velocity-selective ASL	**VSASL**	A general term for ASL techniques where the magnetization is labeled by	(Guo et al., 2015; Qin

		saturation or inversion based on its velocity. See Figure-3 for a general schematic diagram. In the original implementation, the saturation of flowing blood signal is achieved using a double-refocused hyperbolic secant/tangent (DRHS/T) or B_1-Insensitive Rotation-8 (BIR-8) pulse train in combination with velocity encoding gradients. Control images are acquired without velocity encoding gradients.	and van Zijl, 2016; Wong et al., 2006)
Fourier-transform based velocity-selective saturation ASL	**FT-VSS ASL**	A variation of VSASL in which the magnetization within a certain velocity band is saturated by a train of composite pulses incorporating velocity-sensitive bipolar gradients and refocusing 180° pulses. In contrast to the above-mentioned original implementation of VSASL, in FT-VSS-ASL, the static magnetization is saturated while preserving the magnetization flowing above the velocity threshold. In the control image acquisition, all magnetization is saturated.	(Qin et al., 2016; Shin et al., 2013)
Fourier-transform based velocity-selective inversion ASL	**FT-VSI ASL**	Analogous to the FT-VSS ASL method described above, FT-VSI ASL uses composite velocity-selective inversion pulses to invert both flowing and static tissue magnetization (label) or only the static tissue magnetization (control). SNR is improved compared with saturation based VSASL.	(Qin and van Zijl, 2016)
Multi-module Velocity-selective ASL	**mm-VSASL**	A strategy to measure ASL signal with multiple velocity-selective saturation labeling modules to increase labeling	(Guo and Wong, 2015)

		bolus size and reduce T1 relaxation of the ASL signal. This method provides improved SNR compared to conventional single-module VSASL with VS saturation.	
Acceleration-selective ASL	**AccASL**	An extension of VSASL, which labels (saturates) based on the acceleration/deceleration of blood spins rather than their velocity. Since arterial blood exhibits stronger acceleration/deceleration, it labels predominantly arterial (as opposed to venous) blood. AccASL includes both CBF and CBV weighting.	(Schmid et al., 2014)

Subsection 4: Vessel-selective ASL

Name	***Notation***	***Description***	***References***
Vessel-selective ASL		A general term for ASL techniques where blood magnetization of specific targeted arteries is labeled by spatially selective labeling scheme. In general, vessel-selective ASL is achieved by either (P)CASL or PASL.	See each technique below

Subsection 4a: Vessel-selective ASL based on (P)CASL

Name	***Notation***	***Description***	***References***
Oblique-plane CASL / PCASL		The labeling plane is tilted so that it only intersects the arteries of interest, and	(Detre et al., 1994;

		consequently only blood flowing in those arteries is inverted.	Werner et al., 2004)
Rotating oblique plane	**CASSL**	The CASL labeling plane is both tilted and rotating to label only one single artery.	(Helle et al., 2011; Werner et al., 2005)
Vessel-encoded PCASL	**VE-ASL**	Modified PCASL labeling using additional transverse gradients and phase cycling to selectively tag particular arteries. Can use Hadamard vessel encoding or other schemes to generate vascular territory maps.	(Wong, 2007)
Super-selective PCASL	**ss-PCASL**	Creating a labeling disc by incorporating additional variable (rotating) gradients in x and y direction during PCASL labeling to label a single artery.	(Dai et al., 2010; Helle et al., 2010)
Ternary encoded ASL		Encoding super-selective PCASL with a ternary matrix – i.e. a three-fold matrix - without control condition.	(Lindner et al., 2020)

Subsection 4b: Vessel-selective ASL based in PASL

Name	***Notation***	***Description***	***References***
Slab-selective PASL		PASL with anatomically-tilted oblique labeling plane, combined with post-saturation of the imaging volume to remove the direct effects of the labeling pulses on the imaging slices	(Hendrikse et al., 2004)
Pulsed Star Labeling of Arterial Regions	**PULSAR**	Slab-selective STAR labeling, combined with pre-saturation and post-saturation.	(Golay et al., 2005)

Cycled ASL		Slab-selective PASL technique that determines the pattern of label/control acquisition according to a Hadamard matrix. Similar in principle to vessel-encoded PCASL.	(Günther, 2006)

Subsection 5: Multi-time-point Approaches

Name	***Notation***	***Description***	***References***
Multi-time-point ASL		A general term for ASL techniques in which data are acquired repeatedly with varied time parameters (delay time, and/or labeling duration for PCASL) to observe the kinetic ASL signal. Also often called “Multi-delay ASL”, particularly when only the delay time is varied.	
Multi-time-point sequential ASL		Multi-time-point ASL acquisition that acquires images with multiple timepoints as successive single-TI/PLD scans.	
Look-Locker ASL	**LL-ASL**	ASL acquisitions in which several images are acquired at multiple time points after a single labeling module. Readouts with low flip angle are used to reduce saturation of the labeled blood by the first readouts.	(Günther et al., 2001)
Quantitative STAR labeling of arterial regions	**QUASAR**	PASL-based sequence that consists of several Look-Locker readouts: (i) with and without vascular suppression to obtain local arterial input function; (ii) two different readout flip angles. A	(Petersen et al., 2006)

		Q2TIPS-like saturation is used to define the bolus width. This sequence allows measurement of the local AIF and quantification of CBF by deconvolution.	
Reduced resolution transit delay prescan		A fast multi-time point ASL implementation that is specifically used to acquire low spatial resolution arterial transit time maps. Typically used as an ancillary scan to enhance the quantification accuracy of a standard-resolution single-PLD ASL acquisition.	(Dai et al., 2012)
Time-encoded PCASL (also commonly referred to as Hadamard-encoded)	**te-PCASL**	Modification of PCASL which splits the labeling/control module into varying control and label sub-periods according to an encoding matrix. This improves the temporal efficiency of multi-time-point ASL - i.e. reduces the number of acquisitions required for a multi-PLD data set. The most typical implementation is Hadamard encoding. Alternatives include (for example) Walsh-ordering.	(Dai et al., 2013; Guenther, 2007; Teeuwisse et al., 2014; von Samson-Himmelstjerna et al., 2016; Wells et al., 2010)

Subsection 6: MR Fingerprinting ASL

Name	***Notation***	***Description***	***References***
MR fingerprinting ASL	**MRF-ASL**	An ASL method that uses a pseudo-random variation of the acquisition parameters, based on the principles of MR fingerprinting (MRF). Multiple hemodynamic parameters such	(Su et al., 2017; Zhang et al., 2020)

		as B1+, T1, ATT and CBF can be estimated simultaneously.	

Subsection 7: ASL Angiography

ASL-based MR Angiography	**ASL-MRA**	MR Angiography obtained by employing an ASL scheme combined with a high spatial resolution 2D or 3D readout module. Typically, the readout is performed immediately after the labeling while the labeled blood is located within the macro-vasculature. Dynamic MRA is obtainable by using Look-Locker readout or time-encoded ASL scheme. Both PASL and PCASL are suitable for labeling.	(Bi et al., 2010; Suzuki et al., 2020; Yan et al., 2010)
Acquisition of ConTRol and labEled imaging in the Same Shot	**ACTRESS**	Look-locker sampling is performed after ASL labeling and the first phase, in which labeled blood has not yet arrived in the imaging volume, serves as control condition, making the acquisition more efficient	(Suzuki et al., 2018a)
Vessel-selective ASL Angiography		Static or dynamic MRA combined with vessel-selective ASL for visualization of arterial trees arising exclusively from the selected artery(ies).	(Jensen-Kondering et al., 2015; Nakamura et al., 2013; Okell et al., 2010; Robson et al., 2010)
4D dynamic MR angiography using pseudo-continuous arterial spin labeling	**4D-PACK**	PCASL-based 4D dynamic MRA technique which uses keyhole and	(Obara et al., 2018)

combined with Keyhole and View-sharing		view-sharing techniques for scan acceleration.	
Combined ASL and Phase Contrast Angiography		(Super-selective) pseudo-continuous labeling with phase-contrast readout	(Lindner et al., 2017)
Combined ASL angiography and perfusion		A simultaneous acquisition concept in which both angiographic (macro-vasculature) and subsequent perfusion (micro-vasculature) images are obtained by sharing the labeling module within a single ASL sequence.	(Okell, 2019; Suzuki et al., 2018b)
Velocity selective ASL for static MRA	**FT-VSS-MRA**	Static MRA with a FT-VSS ASL labeling scheme, in which the static tissue signal is saturated by FT-VSS, thereby not requiring subtraction.	(Qin et al., 2016; Shin et al., 2013)
Acceleration selective ASL for static MRA	**AccASL-MRA**	Static MRA with the labeling scheme based on AccASL.	(Obara et al., 2017)

Subsection 8: Modified ASL Labeling Methods for Special Derivatives

Name	***Notation***	***Description***	***References***
T2 Relaxation Under Spin Tagging	**TRUST**	A method to measure the cerebral metabolic rate of oxygen ($CMRO_2$). TRUST MRI utilizes the spin tagging principle to label venous blood and uses T2-preparation pulses to modulate the signal with different T2-weightings and thereby measure venous oxygenation.	(Lu and Ge, 2008)
Dual echo ASL BOLD		Acquiring ASL with two echoes, thus being able to extract both ASL and BOLD signals. Recently used to also estimate CMRO2 changes.	(Englund et al., 2020; Fernández-Seara et al., 2016; Glover et al., 1996; Silva et al., 1999)

QUantitative Imaging of eXtraction of Oxygen and TIssue Consumption	**QUIXOTIC**	Method to measure OEF and $CMRO_2$ which uses velocity-selective labeling to isolate MR signal exclusively from postcapillary venular blood. Voxelwise venous oxygenation is estimated via a T2 measurement of the isolated venular blood signal, and OEF and $CMRO_2$ are calculated from this.	(Bolar et al., 2011)
Velocity-Selective Excitation and Arterial Nulling	**VSEAN**	A development of QUIXOTIC which combines velocity-selective excitation and pulsed arterial spin labeling to isolate venular blood signal for venous oxygenation measurement. This method avoids subtraction and associated CSF contamination, and has improved SNR. A T2 measurement of the isolated venular blood signal yields voxelwise venous oxygenation, which can be used to derive OEF and $CMRO_2$.	(Guo and Wong, 2012)
Water extraction with phase contrast arterial spin tagging	**WEPCAST**	A method to measure water extraction fraction. Uses PCASL in combination with phase-contrast velocity-encoding to isolate the ASL signal that passes through into the venous outflow.	(Lin et al., 2018)
Diffusion-weighted ASL	**DW-ASL**	A method which uses vascular crusher gradients to enable acquisition of ASL data with and without the intravascular contribution, and thereby allow estimation of the water exchange rate across the blood-brain barrier..	(Shao et al., 2019a; Wang et al., 2007)
Magnetisation transfer weighted ASL	**MT-ASL**	A method to separate two compartments (capillary and brain tissue) of the ASL signal based on their different magnetisation transfer effects. Water exchange rate across the blood-brain barrier can then be quantified.	(Silva et al., 1997)
Multi-echo time ASL	**Multi-TE ASL**	A method to measure the perfusion signal at a range of echo times, and	(Gregori et al., 2013;

		separate two compartments (capillary and brain tissue) of the ASL signal based on their T2 differences. Water exchange rate across the blood-brain barrier can then be quantified.	Ohene et al., 2019; Schidlowski et al., 2020; Wells et al., 2013)
Intrinsic Diffusivity Encoding of Arterial Labeled Spin	**IDEALS**	A method for whole-brain mapping of water permeability using separation of the intravascular and extravascular signal with segmented 3D-GRASE by modulating the relative sensitivity between relaxation, true diffusion, and pseudo diffusion.	(Wengler et al., 2019)
vascular space occupancy (VASO)-dependent functional MRI (fMRI)	**VASO**	A method predominantly used for fMRI that detects changes in CBV by nulling the blood signal using a flow-independent inversion pulse. Readout is performed when blood signal is zero and the extravascular tissue signal is positive.	(Lu et al., 2003)
inflow Vascular Space Occupancy	**iVASO**	Uses spatially selective inversion to suppress the signal from blood flowing into the imaging volume, with a control scan to measure absolute arterial cerebral blood volume aCBV using cerebrospinal fluid (CSF) for signal normalization.	(Hua et al., 2011a)
Arterial cerebral blood volume-weighted functional MRI using pseudocontinuous arterial spin tagging	**AVAST**	A technique for fast imaging of aCBV signals suitable for functional imaging studies. AVAST was developed in order to achieve a contrast that depends on aCBV with little contamination from perfusion signals by taking advantage of the kinetics of the tag through the vasculature.	(Jahanian et al., 2015)

Section 3: Parameters in ASL Labeling Module

In this section, a list of parameters related to ASL Labeling Methods is provided. This section complies with the consensus paper for brain ASL by the Perfusion Study Group of the International Society for Magnetic Resonance in Medicine (ISMRM) and the EU-COST action 'ASL in dementia' (Alsop et al., 2015), as well as ASL-BIDS. When OSIPI suggests different names/definitions from BIDS, the differences are provided in the description.

Name	***Notation***	***Unit***	***Description***
Labeling duration	LD *Also known as:* τ	ms (OSIPI), sec (BIDS)	For CASL/PCASL. Duration of the constant CASL labeling RF or PCASL labeling pulse train. See Figure-1.
Bolus duration	BD	ms (OSIPI), sec (BIDS)	For PASL. Temporal width of the labeled bolus. For QUIPSS-II/Q2TIPS, this is defined as the time from the labeling pulse to the centre of the first saturation pulse (and is equal to TI_1, see below). If QUIPSS-II/Q2TIPS saturation is not used, this parameter is not known a priori, but is determined by the arterial blood velocity and inversion slab thickness, or the RF transmit coil length for FAIR.
Post-labeling delay	PLD	ms (OSIPI), sec (BIDS)	For CASL/PCASL. Time from the end of the labeling pulse to the center of the imaging excitation pulse (see Figure 1). In a 2D multi-slice acquisition, the PLD is defined by the time of the first slice acquisition; however, it is important to note that the effective PLD for each slice is different, and is determined by the PLD and the inter-slice time.
Inversion time	TI	ms (OSIPI), sec (BIDS)	For general PASL. Time from the center of the labeling pulse to the center of the imaging excitation pulse. In 2D multi-slice acquisition, this relates to the first acquired slice. ASL-BIDS uses the term "post-labeling delay"for this parameter.

Inflow time		ms or s	In some post-processing tools (e.g. FSL), inflow time is used to define the time from the start of labeling to the center of the imaging excitation pulse. For PASL, it is equivalent to inversion time. For PCASL, inflow time is equivalent to PLD + LD.
	TI_1	sec (BIDS), ms (usual)	For QUIPSS-II/Q2TIPS. Time from the center of the labeling pulse to the center of the bolus saturation pulse (QUIPSS-II) or center of the first saturation pulse (Q2TIPS). See Figure-2. ASL-BIDS uses the term "BolusCutOffDelayTime(1)".
	TI_2	ms (OSIPI), sec (BIDS)	For QUIPSS-II/Q2TIPS. Time from the center of the labeling pulse to the center of the excitation pulse of the image acquisition. This value is equivalent to TI of the conventional (non-QUIPSS-II/Q2TIPS) PASL. See Figure-2.
TI_1 stop	TI_{1s}	ms (OSIPI), sec (BIDS)	For Q2TIPS. Time from the center of the labeling pulse to the center of the last bolus saturation pulse. See Figure-2. BIDS uses the term "BolusCutOffDelayTime(2)".
Background suppression (pulse) timing	BS_1 to BS_n	ms or s	The timing parameters for the background suppression RF pulses. Currently, there are three different definitions for these timings implemented on commercial scanners (please see Figure 1): (a) time from the center of either the labeling pulse (for PASL) or the first labeling pulse (for PCASL) to the center of the *n*th background suppression pulse, (b) timing from the center of the *n*th background suppression to the center of the first readout excitation pulse, and (c) BS_n Time: from the center of the last PCASL labeling pulse to the center of the *n*th BS pulse; BS_n TI: from the center of the *n*th BS pulse to the center of the first excitation pulse.

Vascular crusher gradient strength	V_{enc}	cm/s	Crusher gradients have an amplitude sufficient to cause a 180° phase shift for blood moving with a velocity of V_{enc} in the direction of the gradients.
	b	s/mm^2	Crusher gradients are equivalent to diffusion-weighting gradients with this b value (b value defined here: Thomas et al 2000 Phys. Med. Biol. 45 R97 DOI: 10.1088/0031-9155/45/8/201).
Labeling plane			The plane at which flowing blood is labeled in (P)CASL. "Fixed labeling plane" means the labeling plane is parallel to the image slice with a specified distance relative to the lowest slice. "Free labeling plane" means the labeling plane can be moved and angulated independently from the imaging volume
Labeling plane offset / distance		mm	For PCASL, this is the distance between the center of the imaging volume and the center of the labeling plane
Labeling Pulse Average Gradient	G_{av}	mT/m	For PCASL. The non-zero mean gradient applied concurrently with the RF labeling pulses, which combines to produce flow-driven adiabatic inversion. See Figure-4.
Labeling Pulse Maximum Gradient	G_{max}	mT/m	For PCASL. The amplitude of the slice-selection gradient applied during the labeling pulses in the PCASL labeling pulse train. See Figure-4.
Labeling Pulse Average B1	$B1_{av}$	µT	For (P)CASL, the average B1-field strength of the RF labeling pulses over the entire pulse train. See Figure-4.
Labeling Pulse Flip Angle		degree (°)	For PCASL. The flip angle of a single labeling pulse in pCASL labeling pulse train.

Labeling Pulse Interval	Δt	ms	For PCASL. The interval between the centers of two successive PCASL labeling pulses. See Figure-4.
Labeling Pulse Duration	pw δ	ms	For PCASL. The duration of each PCASL labeling pulse. See Figure-4.
PCASL control type			For PCASL. Type of the gradient scheme used in pCASL control condition: either Balanced and Unbalanced. Balanced: Identical G_{av} (nonzero) for label and control. Unbalanced: G_{av} in label is nonzero but zero in control (refocusing gradient lobes are increased in amplitude such that the mean gradient is zero).
Labeling slab			For PASL, the volume over which the labeling RF pulse is applied.
Labeling Slab Thickness		mm	For PASL. The nominal thickness of the labeling RF slab.
Labeling slab gap		mm	For PASL, this is the nominal gap between the leading edge of the labeling slab and the closest edge of the imaging volume
Cutoff velocity	V_{cut}		In VSASL, spins moving above a chosen velocity, referred to as the cutoff velocity (V_{cut}) is labeled. V_{cut} determines how deep into the arterial tree the blood is labeled.

Section 4: Readout Module

Section 5: Derivative Parameters

Subsection 1: Derivative Parameters of Standard ASL

This subsection "Derivative Parameters of Standard ASL" complies with the consensus paper for brain ASL by the Perfusion Study Group of the International Society for Magnetic Resonance in Medicine (ISMRM) and the EU-COST action 'ASL in dementia' (Alsop et al., 2015), as well as ASL-BIDS Extension Proposal which is currently being developed.

Name	***Notation***	***Unit***	***Description***
ASL difference image *Also known as* *Delta M* Perfusion weighted image	ΔM	arbitrary unit	Image obtained by subtracting the labeled image from the control image, which subtracts out the static tissue signal and consequently shows the perfusion signal produced by ASL preparation.
Normalised perfusion weighted image	ΔM/M0	%	ASL difference image normalized by M0, expressed as a percentage.
Cerebral Blood Flow	CBF	mL/100g/min	Quantity of blood (mL) reaching 100g of brain tissue per unit of time (min)
Arterial Transit Time *Also known as:* Bolus Arrival Time Arterial Arrival Time	**ATT** BAT AAT	ms	Time between when blood is labeled and when it first arrives in the imaging voxel/slice. Note that ATT, AAT and BAT are dependent on the positioning of the labeling plane/slab relative to the imaging volume, and are therefore not generally comparable across studies.

Subsection 2: Derivative Parameters of Advanced ASL

Name	*Notation*	*Unit*	*Description*	*References*
Tissue transit time	**TTT** or $\boldsymbol{\delta}$	ms	TTT is the time between the spins being labeled and arriving in the tissue compartment (after being transported from capillary to tissue).	(Alsop and Detre, 1996) (Wang et al., 2002)
Pre-exchange lifetime, or mean blood water residence time, or mean exchange time	**T_{ex} or** τ_e	ms	The difference between TTT and ATT i.e. the time between arrival of labeled blood in the voxel and exchange from the blood into the extravascular tissue	(Wells et al., 2013) (Dickie et al., 2020)
Delivery function Fractional arterial input function	**c(t)**	fraction (0 to 1)	Fractional ASL signal in larger arteries. Corresponds to the normalized arterial concentration of magnetization arriving at the voxel at time t, and is subject to T1 decay. Its shape depends on the labeling type.	(Buxton et al., 1998) (Petersen et al., 2006) (Knutsson et al., 2008)
Arterial input function	**AIF**	arbitrary unit	Describes inflowing magnetization and is obtained by multiplication of the delivery function c(t) by $2M_{0b}$.	(Petersen et al., 2006) (Knutsson et al., 2008)
Equilibrium water exchange rate from capillary to tissue	**k_{in} or k_w**	min^{-1}	Water exchange rate across the blood-brain barrier, which is mediated by multiple pathways including passive diffusion through endothelium, active cotransport (i.e. via ion channels), and through	(Parkes and Tofts, 2002) (Wang et al., 2007) (St. Lawrence et al., 2012)

			water channel proteins (aquaporin-4) at the end feet of astrocytes. This exchange rate can be quantified by separating the signal contributions from the capillary and tissue compartments.	(Gregori et al., 2013) (Dickie et al., 2020)
Arterial blood flow (through a unit volume)	**aBF**	mL/mL/min	Arterial blood flow per unit volume in large arteries can be quantified using model-free methods under the assumption of indicator-dilution theory from dynamic MR angiography with sufficient spatial and temporal resolution.	(Shao et al., 2019) (Shao et al., 2019b)
Arterial blood volume / Arterial cerebral blood volume	**aBV / aCBV / CBV_a**	fraction (0 to 1) or % or ml blood /100 ml tissue	Ratio of the intravascular volume of arteries and arterioles to the entire voxel volume	(Barbier et al., 2001; Brookes et al., 2007; Hua et al., 2011b; Petersen et al., 2006; Yan et al., 2012)
Partial (capillary, intravascular, extravascular) volume fraction	**V_c** **V_i** **V_e**	**mL/100 g**	Distribution volume of labeled blood in the capillary, intravascular, or extravascular space	(Gregori et al., 2013; Shao et al., 2019a; St Lawrence and Lee, 1998)
Water extraction fraction	**E_w** **EF**	**fraction (0 to 1)**	Fraction of water that is extracted into the extravascular space	(Shao et al., 2019a; St Lawrence and Lee, 1998)
Permeability surface area product of water	**PS_w**	**mL/min/ 100 g**	Capillary permeability surface-area product, measuring water flow through the vessel wall per unit volume	(Gregori et al., 2013; Shao et al., 2019a; St

				Lawrence and Lee, 1998)
Volume flow rate	**Q**	**mL/min**	Volume of blood passing through an artery per unit time, which can be obtained by multiplication of the artery cross section with mean velocity, or by ASL-MRA.	(Okell et al., 2013; van Osch et al., 2006)
Vascular compliance	**VC**	ml/mmHg	VC is defined as the ratio of change in arterial cerebral blood volume (ΔCBV) and change in arterial pressure (ΔBP) between the systolic and diastolic phases of the cardiac cycle. ΔCBV can be measured by synchronized dynamic ASL.	(Yan et al., 2016)
Cerebrovascular reactivity	**CVR(*)**	ΔCBF(%) ΔCBF(%)/mm Hg	CVR is a measure of the change in cerebral blood flow for a given vasodilatory stimulus (i.e CO2, acetazolamide). Often, this is normalized to the change in end-tidal CO_2.	(Tancredi et al., 2012)
Cerebrovascular reserve	**CVR**	%	The maximum possible change in CBF from baseline due to stimulation	(Ozgur et al., 2001)

*Please note that, in general, the same notation “CVR” is used for both cerebrovascular reactivity and cerebrovascular reserve.

Subsection 3: Derivative Parameters in Partial Volume Correction

$$CBF = pGM \cdot CBF_{GM} + pWM \cdot CBF_{WM}$$

(Asllani et al., 2008)

Name	*Notation*	*Unit*	*Description*	*References*
Partial volume effect	PVE		The typical voxel size of an ASL perfusion image is much larger than the cortical thickness, and individual voxels are likely to contain a mixture of gray matter (GM), white matter (WM), and cerebrospinal fluid (CSF), which is known as the partial volume effect.	(Asllani et al., 2008; Chappell et al., 2011)
Tissue partial volume *Also known as:* Fractional tissue volume	P_{GM}, P_{WM}, P_{CSF}	Fraction (0 to 1)	Partial volume of different tissue types (GM, WM, CSF) as a fraction of the total voxel volume	(Asllani et al., 2008)
Tissue specific perfusion	CBF_{GM} CBF_{WM}		Perfusion, of specific tissue types within a voxel, estimated either by (a) including only voxels with a tissue probability value higher than a stated threshold, or (b) explicitly correcting for the partial volume effects of GM/WM/CSF within voxels.	(Asllani et al., 2008; Chappell et al., 2011)

Section 6: Ancillary parameters for quantification

Subsection 1: One-compartment model for single-PLD

The general kinetic model is used to derive the quantification equations below. Several assumptions need to be fulfilled to ensure its validity - for example delivery of the entire

bolus to the tissue and that label relaxation is governed by blood T1 during the entire measurement. This is the basic quantification model recommended by the ASL consensus paper (Alsop et al., 2015).

PCASL

$$\mathrm{CBF} = \frac{6000 \cdot \lambda \cdot \Delta M \cdot e^{\frac{\mathrm{PLD}}{T_{1b}}}}{2 \cdot \alpha \cdot T_{1b} \cdot M_{0t} \cdot \left(1 - e^{-\frac{\tau}{T_{1b}}}\right)} [\mathrm{mL/min/100g}]$$

(Alsop et al., 2015; Buxton et al., 1998)

PASL

$$\mathrm{CBF} = \frac{6000 \cdot \lambda \cdot \Delta M \cdot e^{\frac{\mathrm{TI}}{T_{1b}}}}{2 \cdot \alpha \cdot TI_1 \cdot M_{0t}} [\mathrm{mL/min/100g}]$$

(Alsop et al., 2015; Wong et al., 1998a)

Name	***Notation***	***Unit***	***Description***	***Literature value***	***References***
T1 relaxation time of blood *Also known as:* Blood T1	**T_{1b}**	**ms**	The longitudinal relaxation time of arterial blood	**ASL White paper consensus:** 1.5T: 1350 ms	(Lu et al., 2003)
				3T: 1650 ms	(Lu et al., 2004)
				Renal consensus: 1.5T: 1480 ms	(Nery et al., 2020)
				Other sources: 1.5T: 1480 ms 3.0T: 1649 ms 3.0T: 1842 ms 7.0T: 2087 ms 7.0T: 2212 ms 9.4T: 2429 ms	(Dobre et al., 2007; Zhang et al., 2013; Li et al., 2017)

Equilibrium magnetization of blood *Also known as:* M_0 of blood	M_{0b}	arbitrary unit	Fully relaxed longitudinal magnetization of arterial blood, which is required to scale the subtracted ASL signal and obtain absolute CBF units. In the ASL White paper, it is recommended to estimate M_{0b} voxel-wise from M_{0t} measured by an M_0 image. The blood-brain partition coefficient λ scales M_{0t} to M_{0b}.	N.A.	(Alsop et al., 2015)
Equilibrium magnetization of tissue *Also known as:* M_0 of tissue	M_{0t}	arbitrary unit	Fully relaxed longitudinal magnetization of tissue. This value might be different in different organs or tissue types with an organ.	N.A.	(Alsop et al., 2015)
Blood-brain partition coefficient	λ	**mL/g**	The ratio between blood and tissue water concentration at equilibrium in mL of blood, per g of tissue. When used in ASL quantification, instantaneous equilibrium between tissue and veins is assumed	Whole brain average: 0.9 Gray matter: 0.98 White matter: 0.82	(Herscovitch and Raichle, 1985)
Labeling efficiency	α	**fraction (0 to 1)**	Combines the inversion efficiency of the labeling pulse itself and the loss of label caused by	Labeling pulse PCASL: 0.85 PASL: 0.98	(Dai et al., 2008; Garcia et al., 2005; Wong et al., 1998b)

			background suppression (dependent on the number and type of BS pulses). A value of 1 corresponds to full inversion of blood magnetization.	Background Suppression (per pulse): 0.93	

Subsection 2: Haematocrit

Blood T1 relaxation time depends on the hematocrit level and can differ across populations, disease, and sex. It is advised to measure the T_{1b} if heterogeneous Hct values are expected in the population. An alternative is to estimate T_{1b} from the Hct values obtained from blood samples.

Adult (simplified, 3T)

$$T_{1b} = \frac{1}{0.52 \cdot \mathrm{Hct} + 0.38}[\mathrm{s}]$$

(Lu et al., 2004)

Adult

$$T_{1b} = \frac{1}{f_e \cdot [0.603 - 0.034 \cdot B_0 + 0.033 \cdot Hb \cdot (1 - Y)] + 0.496 - 0.023 \cdot B_0} + \Delta T_{1b}[s]$$

$$f_e = \frac{0.7 \cdot \mathrm{Hct}}{0.7 \cdot \mathrm{Hct} + 0.95 \cdot (1 - \mathrm{Hct}))}$$

(Hales et al., 2016)

Neonates (simplified, 3T)

$$T_{1b} = \frac{1}{0.5 \cdot \mathrm{Hct} + 0.37}[\mathrm{s}]$$

(De Vis et al., 2014)

Name	***Notation***	***Unit***	***Description***	***Literature value***	***References***

Hematocrit	**Hct**	**fraction (0 to 1)**	Ratio of the volume of red blood cells to the total volume of blood	Adult: 0.38 –0.46 Neonate: 0.28–0.67	(Lu et al., 2004) (De Vis et al., 2014)
Water fraction in erythrocytes	**f_e**	**fraction (0 to 1)**	The fraction of water in whole blood that resides in erythrocytes. Calculated based on the hematocrit value.		(Hales et al., 2016)
Hemoglobin concentration	**ctHb**	**g/dL**	Total concentration of hemoglobin in blood.	12.9 - 15.6	(Grgac et al., 2013)
Oxygen saturation	**Y**	**fraction (0 to 1)**	Oxygen saturation fraction (0-1). Default value for arterial blood is used if not measured	Arteries: 0.97 Capillaries: 0.77	(Hales et al., 2016) (Zhao et al., 2007)
Difference between predicted and measured T_{1b}	**ΔT_{1b}**	**s**	The difference between the predicted and measured values calculated as the mean bias in the in-vivo literature values	In-vitro: 0 s In-vivo: 0.108 s	(Hales et al., 2016)

Subsection 3: Advanced physiological parameters

Name	***Notation***	***Unit***	***Description***	***Literature value***	***References***
Flow velocity	**v** **u**	**cm/s**	Flow velocity of blood in the feeding arteries. It directly influences the labeling efficiency in pCASL		

Section 7: Outside of Brain

Subsection 1: Derivative Parameters in Body

Organ	Name	*Notation*	*Unit*	*Description*	*References*
Placenta	Placental Blood Flow / Placental perfusion	PBF	mL/100g/min	Perfusion value in placenta	(Shao et al., 2018) (Zun and Limperopoulos, 2018)
Kidney	Renal Blood Flow / Renal perfusion	RBF	mL/100g/min	Tissue perfusion value in kidney	(Nery et al., 2018) (Odudu et al., 2018)
Liver	Hepatic arterial perfusion		mL/100g/min	Perfusion arising from the hepatic arteries in liver	(Schalkx et al., 2015) (Pan et al., 2016) (Martirosian et al., 2019)
	Portal-venous perfusion		mL/100g/min	Perfusion arising from the portal veins in liver	
	Hepatic perfusion index	HPI	%	Percentage ratio of the hepatic arterial perfusion to the global liver perfusion	
Heart	Myocardial blood flow	MBF	mL/100g/min	Perfusion value in myocardium	(Kober et al., 2016)
	Myocardial perfusion reserve	MPR		MPR was defined as the ratio of MBF at stress (i.e. using adenosine vasodilation) and at rest.	(Yoon et al., 2017) (Aramendía-Vidaurreta et al., 2020)

Subsection 2: Organ Specific Parameters in Body

	λ (mL/g)	***T1t (ms)***	***Reference***
Kidney cortex	0.9	966±58 (1.5T) 1142±154 (3T)	(Nery, et al. 2020) (Gardener, et al. 2010) (de Bazelaire, et al. 2004) (Roberts, et al. 1995)
Kidney medulla	0.9	1412±58 (1.5T) 1545±142 (3T)	(Nery, et al. 2020) (Gardener, et al. 2010) (de Bazelaire, et al. 2004) (Roberts, et al. 1995)
Thyroid	0.8	1000 (1.5T)	(Schraml, et al. 2007)
Parotid gland	1.0	800 (1.5T)	(Schwenzer, et al. 2008) (de Bazelaire, et al. 2004) (Mascaro, et al. 1995)
Placenta	0.9	1684 (1.5T), negative corr. with gestational age	(Zun, et al. 2017) (Wright, et al. 2013)
Liver		586±39 (1.5T) 809±71 (3T)	(de Bazelaire, et al. 2004)
Spleen		1057±42 (1.5T) 1328±31 (3T)	(de Bazelaire, et al. 2004)
Pancreas		584±14 (1.5T) 725±71 (3T)	(de Bazelaire, et al. 2004)
Paravertebral muscle		856±61 (1.5T) 898±33 (3T)	(de Bazelaire, et al. 2004)
Bone marrow (L4)		549±52 (1.5T) 586±73 (3T)	(de Bazelaire, et al. 2004)
Subcutaneous fat		343±37 (1.5T) 382±13 (3T)	(de Bazelaire, et al. 2004)

Prostate		1317±85 (1.5T) 1597±42 (3T)	(de Bazelaire, et al. 2004)
Myometrium		1309±35 (1.5T) 1514±156 (3T)	(de Bazelaire, et al. 2004)
Endometrium		1274±64 (1.5T) 1453±123 (3T)	(de Bazelaire, et al. 2004)
Cervix		1135±154 (1.5T) 1616±61 (3T)	(de Bazelaire, et al. 2004)
Myocardium	0.92	1158 (3T)	(Bergmann, et al. 1984) (von Knobelsdorff-Brenkenhoff et al. 2013)

Figures

Figure 1

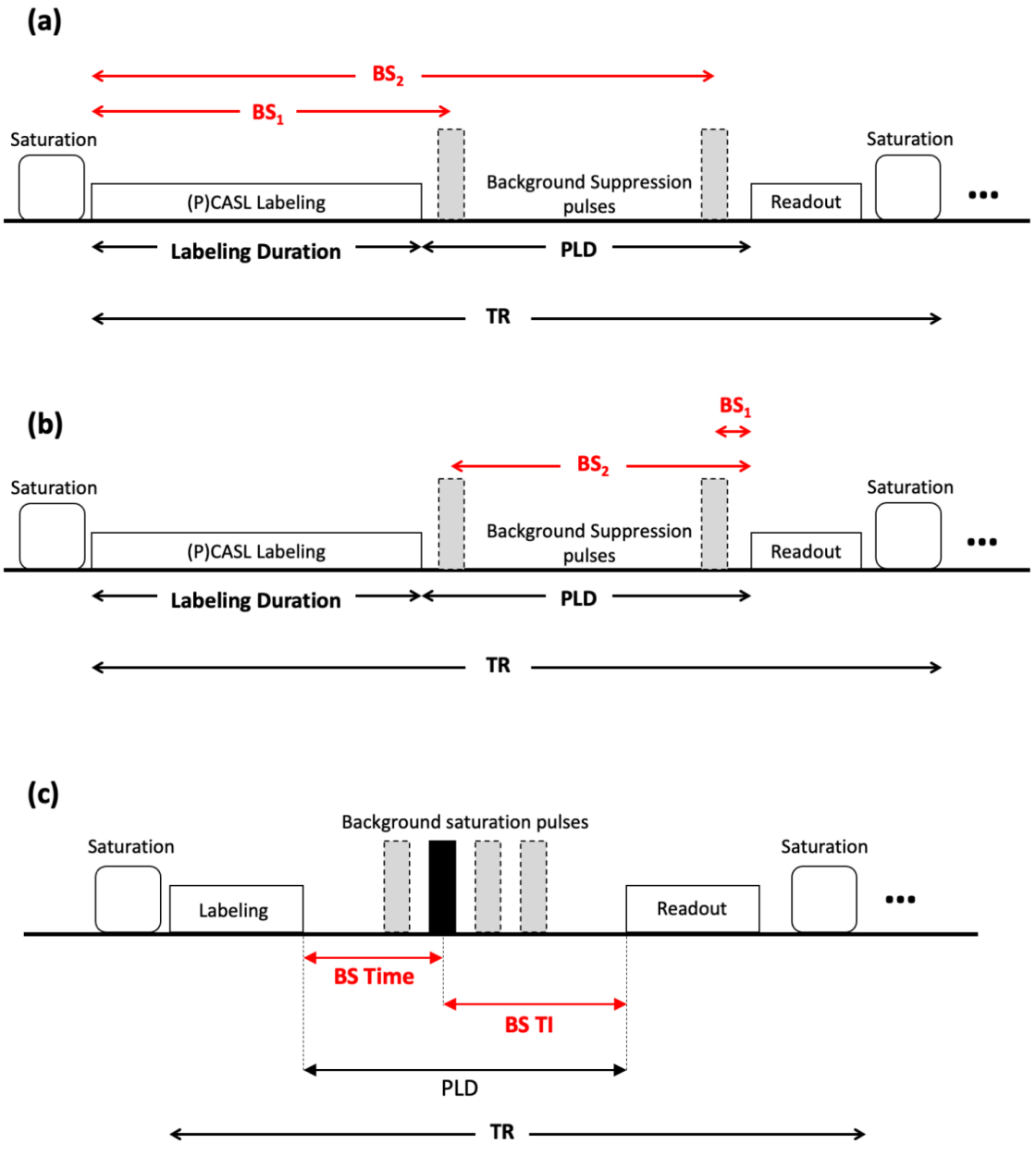

Figure 1: Schematic sequence diagram of (P)CASL.

The timing parameter for the background suppression (BS) pulses. Currently, there are three different definitions of the timings implemented in commercial scanners: (a) time from the center of the first PCASL labeling pulse to the center of the *n*th BS pulse, (b) time from the center of the first excitation pulse to the centre of the *n*th BS pulse, (c) BS Time: from the center of the last PCASL labeling pulse to the center of the *n*th BS pulse; BS TI: from the center of the *n*th BS pulse to the center of the first excitation pulse. (Figure (c) courtesy: Canon Medical Systems Corporation).

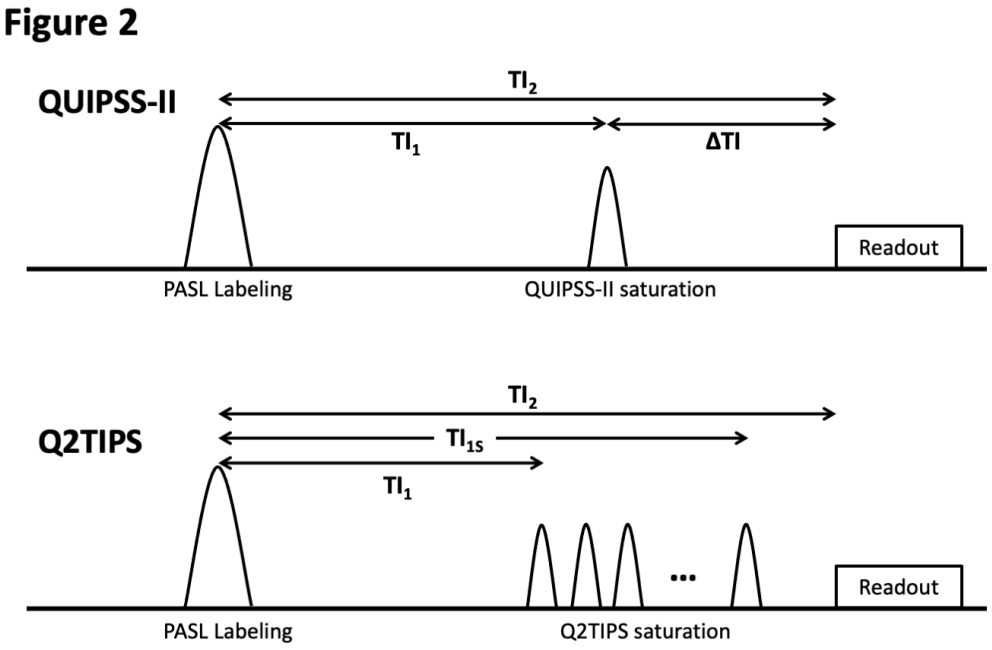

Figure 2: Schematic sequence diagram of QUIPSS-II and Q2TIPS.

Figure 3

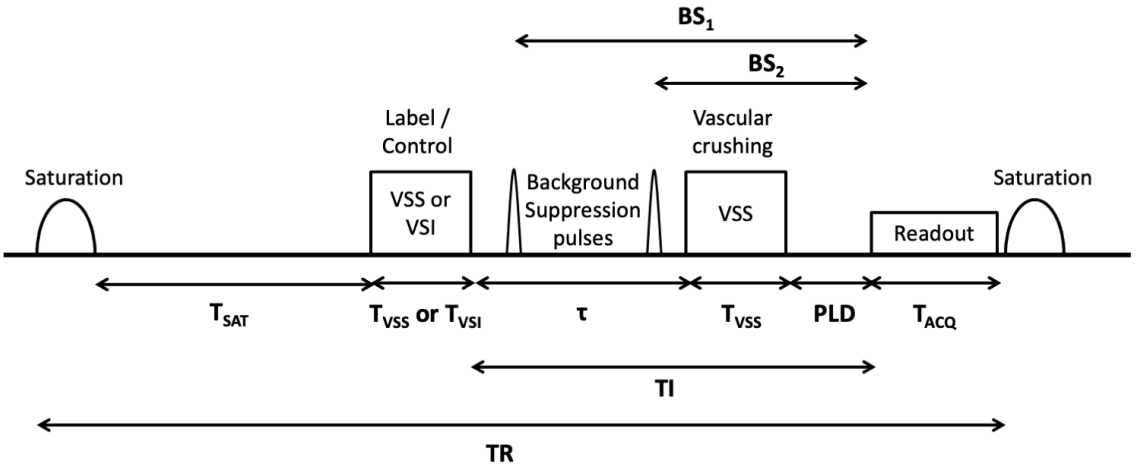

Figure 3: Schematic sequence diagram of Velocity-selective (VS-) ASL.

Figure 4

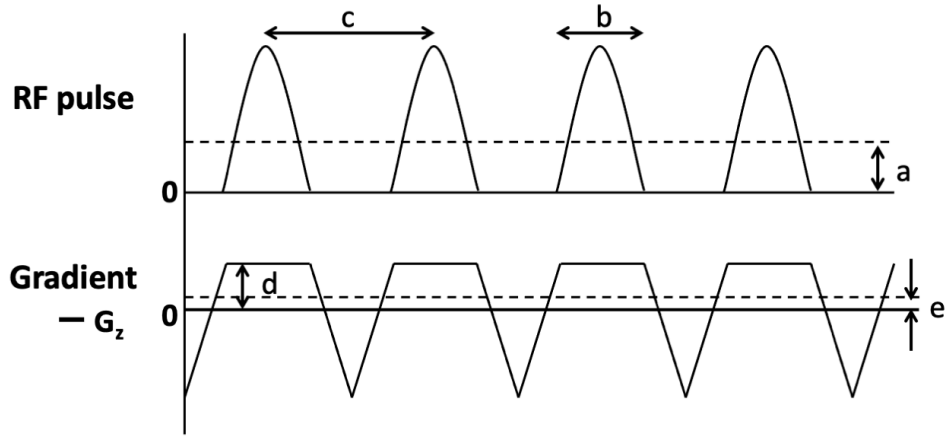

a: Labeling Pulse Average B1
b: Labeling Pulse Duration
c: Labeling Pulse Interval
d: Labeling Pulse Maximum Gradient
e: Labeling Pulse Average Gradient

Figure 4: Schematic diagram of PCASL labeling pulse train.

Part 2: Reporting Recommendations

Section 1: Parameters in "Required" category

In this section, a list of parameters in "Required category" is provided, which are essential for meaningful interpretation of the ASL data and for quantitative analysis. These must be included in an ASL publication in order for its data set to be 'OSIPI compliant'.

Name	***Abbreviation***	***Style***	***Condition***
General			
Arterial Spin Labeling Type		PASL, (P)CASL, Velocity-selective, etc.	
Background Suppression	BS/BGS	Yes/No	
Method for M_{0b} estimation		The description of how M_{0b} is estimated, e.g. how the M_0 image is acquired, or any special method to estimate M_{0b} directly	When CBF estimation is performed
Total acquired pairs		The number of paired labeled and control images, before online averaging is performed (if applicable)	
Acquisition Voxel Size		Value in mm	
(P)CASL			
Labeling duration	LD / τ	Value in ms or s	
Post-labeling delay	PLD	Value in ms or s	
PASL			
Inversion time / Inflow time	TI	Value in ms	

Bolus cut-off techniques		Name of technique, or None	
	TI_1	Value in ms	When QUIPSS-II or Q2TIPS are used.
	TI_2	Value in ms	When QUIPSS-II or Q2TIPS are used.
	TI_{1s}	Value in ms	When Q2TIPS is used.

Section 2: Parameters in "Recommended" category

In this section, a list of parameters in "Recommended category" is provided, which are useful for interpretation of the ASL data and could explain specific characteristics or systematic differences between data sets. We encourage authors to include as many of these as possible in ASL publications.

Name	***Abbreviation***	***Style***	***Condition***
General			
Number of background suppression pulse		Value	If BS is used and details are available to user.
Background suppression (pulse) timing	BS_1 to BS_n or BS Time/TI	Value in ms	If BS is used and details are available to the user
Background suppression timing definition		The description of how timing is defined. See "Background suppression (pulse) timing" in Section 3, or Figure 1.	If BS is used and details are available to the user
Labeling Location Description		Description of the labeling plane/slab location (other factor than offset/gap), such as the planning of the labeling	

		plane/slab with respect to the imaging slices	
Shim volume		Description of shim volume used: imaging volume only, both imaging volume and labeling region, labeling region during labeling pulse and imaging volume during acquisition, or other (please specify)	
Vascular crushing	V_{enc}	Value in cm/s	When Vascular crushing is performed. Ideally, both V_{enc} and b should be specified.
	b	value in s/mm^2	
(P)CASL			
PCASL control type		Balanced or Unbalanced	
CASL type		If a separate coil is used for labeling	
Labeling plane offset / distance		Value in mm	
Labeling Pulse Average Gradient	G_{av}	Value in mT/m	When details are available to the user
Labeling Pulse Maximum Gradient	G_{max}	Value in mT/m	When details are available to the user
Labeling Pulse Average B1	$B1_{av}$	Value in µT	When details are available to the user
Labeling Pulse Flip Angle		Value in degree (°)	When details are available to the user
Labeling Pulse Interval	TR_{PCASL}	Value in ms	When details are available to the user

Labeling Pulse Duration	pw	Value in ms	When details are available to the user
PASL			
PASL type		EPISTAR, FAIR, PICORE, etc	
Labeling slab thickness		Value in mm	
Labeling slab gap		Value in mm	

References

Alsop, D.C., Detre, J.A., 1998. Multisection cerebral blood flow MR imaging with continuous arterial spin labeling. Radiology 208, 410–416. https://doi.org/10.1148/radiology.208.2.9680569

Alsop, D.C., Detre, J.A., 1996. Reduced transit-time sensitivity in noninvasive magnetic resonance imaging of human cerebral blood flow. J. Cereb. Blood Flow Metab. Off. J. Int. Soc. Cereb. Blood Flow Metab. 16, 1236–1249. https://doi.org/10.1097/00004647-199611000-00019

Alsop, D.C., Detre, J.A., Golay, X., Günther, M., Hendrikse, J., Hernandez-Garcia, L., Lu, H., MacIntosh, B.J., Parkes, L.M., Smits, M., van Osch, M.J.P., Wang, D.J.J., Wong, E.C., Zaharchuk, G., 2015. Recommended implementation of arterial spin-labeled perfusion MRI for clinical applications: A consensus of the ISMRM perfusion study group and the European consortium for ASL in dementia. Magn. Reson. Med. 73, 102–116. https://doi.org/10.1002/mrm.25197

Asllani, I., Borogovac, A., Brown, T.R., 2008. Regression algorithm correcting for partial volume effects in arterial spin labeling MRI. Magn. Reson. Med. 60, 1362–1371. https://doi.org/10.1002/mrm.21670

Barbier, E.L., Silva, A.C., Kim, S.G., Koretsky, A.P., 2001. Perfusion imaging using dynamic arterial spin labeling (DASL). Magn. Reson. Med. 45, 1021–1029. https://doi.org/10.1002/mrm.1136

Barker, P.B., Golay, X., Zaharchuk, G. (Eds.), 2013. Clinical Perfusion MRI: Techniques and Applications. Cambridge University Press, Cambridge. https://doi.org/10.1017/CBO9781139004053

Bi, X., Weale, P., Schmitt, P., Zuehlsdorff, S., Jerecic, R., 2010. Non-contrast-enhanced four-dimensional (4D) intracranial MR angiography: A feasibility study. Magn. Reson. Med. 63, 835–841. https://doi.org/10.1002/mrm.22220

Bolar, D.S., Rosen, B.R., Sorensen, A.G., Adalsteinsson, E., 2011. QUantitative Imaging of eXtraction of oxygen and TIssue consumption (QUIXOTIC) using venular-targeted velocity-selective spin labeling. Magn. Reson. Med. 66, 1550–1562. https://doi.org/10.1002/mrm.22946

Brookes, M.J., Morris, P.G., Gowland, P.A., Francis, S.T., 2007. Noninvasive measurement of arterial cerebral blood volume using Look-Locker EPI and arterial spin labeling. Magn. Reson. Med. 58, 41–54. https://doi.org/10.1002/mrm.21199

Buxton, R.B., Frank, L.R., Wong, E.C., Siewert, B., Warach, S., Edelman, R.R., 1998. A general kinetic model for quantitative perfusion imaging with arterial spin labeling. Magn. Reson. Med. 40, 383–396. https://doi.org/10.1002/mrm.1910400308

Chappell, M.A., Groves, A.R., MacIntosh, B.J., Donahue, M.J., Jezzard, P., Woolrich, M.W., 2011. Partial volume correction of multiple inversion time arterial spin labeling MRI data. Magn. Reson. Med. 65, 1173–1183. https://doi.org/10.1002/mrm.22641

Dai, W., Garcia, D., de Bazelaire, C., Alsop, D.C., 2008. Continuous flow-driven inversion for arterial spin labeling using pulsed radio frequency and gradient fields. Magn. Reson. Med. 60, 1488–1497. https://doi.org/10.1002/mrm.21790

Dai, W., Robson, P.M., Shankaranarayanan, A., Alsop, D.C., 2012. Reduced resolution transit delay prescan for quantitative continuous arterial spin labeling perfusion imaging. Magn. Reson. Med. 67, 1252–1265. https://doi.org/10.1002/mrm.23103

Dai, W., Robson, P.M., Shankaranarayanan, A., Alsop, D.C., 2010. Modified pulsed continuous arterial spin labeling for labeling of a single artery. Magn. Reson. Med. 64, 975–982. https://doi.org/10.1002/mrm.22363

Dai, W., Shankaranarayanan, A., Alsop, D.C., 2013. Volumetric measurement of perfusion and arterial transit delay using hadamard encoded continuous arterial spin labeling. Magn. Reson. Med.

69, 1014–1022. https://doi.org/10.1002/mrm.24335
De Vis, J.B., Hendrikse, J., Groenendaal, F., de Vries, L.S., Kersbergen, K.J., Benders, M.J.N.L., Petersen, E.T., 2014. Impact of neonate haematocrit variability on the longitudinal relaxation time of blood: Implications for arterial spin labelling MRI. NeuroImage Clin. 4, 517–525. https://doi.org/10.1016/j.nicl.2014.03.006
Detre, J.A., Zhang, W., Roberts, D.A., Silva, A.C., Williams, D.S., Grandis, D.J., Koretsky, A.P., Leigh, J.S., 1994. Tissue specific perfusion imaging using arterial spin labeling. NMR Biomed. 7, 75–82. https://doi.org/10.1002/nbm.1940070112
Dobre, M.C., Uğurbil, K., Marjanska, M., 2007. Determination of blood longitudinal relaxation time (T1) at high magnetic field strengths. Magn. Reson. Imaging 25, 733–735. https://doi.org/10.1016/j.mri.2006.10.020
Edelman, R.R., Chen, Q., 1998. EPISTAR MRI: Multislice mapping of cerebral blood flow. Magn. Reson. Med. 40, 800–805. https://doi.org/10.1002/mrm.1910400603
Englund, E.K., Fernández-Seara, M.A., Rodríguez-Soto, A.E., Lee, H., Rodgers, Z.B., Vidorreta, M., Detre, J.A., Wehrli, F.W., 2020. Calibrated fMRI for dynamic mapping of CMRO2 responses using MR-based measurements of whole-brain venous oxygen saturation. J. Cereb. Blood Flow Metab. 40, 1501–1516. https://doi.org/10.1177/0271678X19867276
Fernández-Seara, M.A., Rodgers, Z.B., Englund, E.K., Wehrli, F.W., 2016. Calibrated bold fMRI with an optimized ASL-BOLD dual-acquisition sequence. NeuroImage 142, 474–482. https://doi.org/10.1016/j.neuroimage.2016.08.007
Garcia, D.M., Duhamel, G., Alsop, D.C., 2005. Efficiency of inversion pulses for background suppressed arterial spin labeling. Magn. Reson. Med. 54, 366–372. https://doi.org/10.1002/mrm.20556
Glover, G.H., Lemieux, S.K., Drangova, M., Pauly, J.M., 1996. Decomposition of inflow and blood oxygen level-dependent (BOLD) effects with dual-echo spiral gradient-recalled echo (GRE) fMRI. Magn. Reson. Med. 35, 299–308. https://doi.org/10.1002/mrm.1910350306
Golay, X., Hendrikse, J., Lim, T.C.C., 2004. Perfusion imaging using arterial spin labeling. Top. Magn. Reson. Imaging TMRI 15, 10–27. https://doi.org/10.1097/00002142-200402000-00003
Golay, X., Petersen, E.T., Hui, F., 2005. Pulsed star labeling of arterial regions (PULSAR): A robust regional perfusion technique for high field imaging. Magn. Reson. Med. 53, 15–21. https://doi.org/10.1002/mrm.20338
Golay, X., Stuber, M., Pruessmann, K.P., Meier, D., Boesiger, P., 1999. Transfer insensitive labeling technique (TILT): Application to multislice functional perfusion imaging. J. Magn. Reson. Imaging 9, 454–461. https://doi.org/10.1002/(SICI)1522-2586(199903)9:3<454::AID-JMRI14>3.0.CO;2-B
Gorgolewski, K.J., Auer, T., Calhoun, V.D., Craddock, R.C., Das, S., Duff, E.P., Flandin, G., Ghosh, S.S., Glatard, T., Halchenko, Y.O., Handwerker, D.A., Hanke, M., Keator, D., Li, X., Michael, Z., Maumet, C., Nichols, B.N., Nichols, T.E., Pellman, J., Poline, J.-B., Rokem, A., Schaefer, G., Sochat, V., Triplett, W., Turner, J.A., Varoquaux, G., Poldrack, R.A., 2016. The brain imaging data structure, a format for organizing and describing outputs of neuroimaging experiments. Sci. Data 3, 160044. https://doi.org/10.1038/sdata.2016.44
Gregori, J., Schuff, N., Kern, R., Günther, M., 2013. T2-based arterial spin labeling measurements of blood to tissue water transfer in human brain. J. Magn. Reson. Imaging JMRI 37, 332–342. https://doi.org/10.1002/jmri.23822
Grgac, K., van Zijl, P.C.M., Qin, Q., 2013. Hematocrit and oxygenation dependence of blood (1)H(2)O T(1) at 7 Tesla. Magn. Reson. Med. 70, 1153–1159. https://doi.org/10.1002/mrm.24547

Guenther, M., 2007. Highly Efficient Accelerated Acquisition of Perfusion Inflow Series by Cycled Arterial Spin Labeling 1.

Günther, M., 2006. Efficient visualization of vascular territories in the human brain by cycled arterial spin labeling MRI. Magn. Reson. Med. 56, 671–675. https://doi.org/10.1002/mrm.20998

Günther, M., Bock, M., Schad, L.R., 2001. Arterial spin labeling in combination with a look-locker sampling strategy: Inflow turbo-sampling EPI-FAIR (ITS-FAIR). Magn. Reson. Med. 46, 974–984. https://doi.org/10.1002/mrm.1284

Guo, J., Meakin, J.A., Jezzard, P., Wong, E.C., 2015. An optimized design to reduce eddy current sensitivity in velocity-selective arterial spin labeling using symmetric BIR-8 pulses. Magn. Reson. Med. 73, 1085–1094. https://doi.org/10.1002/mrm.25227

Hales, P.W., Kirkham, F.J., Clark, C.A., 2016. A general model to calculate the spin-lattice (T1) relaxation time of blood, accounting for haematocrit, oxygen saturation and magnetic field strength. J. Cereb. Blood Flow Metab. Off. J. Int. Soc. Cereb. Blood Flow Metab. 36, 370–374. https://doi.org/10.1177/0271678X15605856

Helle, M., Norris, D.G., Rüfer, S., Alfke, K., Jansen, O., van Osch, M.J., 2010. Superselective pseudocontinuous arterial spin labeling. Magn. Reson. Med. 64, 777–786.

Helle, M., Rüfer, S., Alfke, K., Jansen, O., Norris, D.G., 2011. Perfusion territory imaging of intracranial branching arteries – optimization of continuous artery-selective spin labeling (CASSL). NMR Biomed. 24, 404–412. https://doi.org/10.1002/nbm.1605

Hendrikse, J., van der Grond, J., Lu, H., van Zijl, P.C.M., Golay, X., 2004. Flow territory mapping of the cerebral arteries with regional perfusion MRI. Stroke 35, 882–887. https://doi.org/10.1161/01.STR.0000120312.26163.EC

Herscovitch, P., Raichle, M.E., 1985. What is the correct value for the brain--blood partition coefficient for water? J. Cereb. Blood Flow Metab. Off. J. Int. Soc. Cereb. Blood Flow Metab. 5, 65–69. https://doi.org/10.1038/jcbfm.1985.9

Hua, J., Qin, Q., Donahue, M.J., Zhou, J., Pekar, J.J., van Zijl, P.C.M., 2011a. Inflow-based vascular-space-occupancy (iVASO) MRI. Magn. Reson. Med. 66, 40–56. https://doi.org/10.1002/mrm.22775

Hua, J., Qin, Q., Pekar, J.J., van Zijl, P.C.M., 2011b. Measurement of absolute arterial cerebral blood volume in human brain without using a contrast agent. NMR Biomed. 24, 1313–1325. https://doi.org/10.1002/nbm.1693

Jahanian, H., Peltier, S., Noll, D.C., Hernandez Garcia, L., 2015. Arterial cerebral blood volume-weighted functional MRI using pseudocontinuous arterial spin tagging (AVAST). Magn. Reson. Med. 73, 1053–1064. https://doi.org/10.1002/mrm.25220

Jahng, G.-H., Zhu, X.-P., Matson, G.B., Weiner, M.W., Schuff, N., 2003. Improved perfusion-weighted MRI by a novel double inversion with proximal labeling of both tagged and control acquisitions. Magn. Reson. Med. 49, 307–314. https://doi.org/10.1002/mrm.10339

Jensen-Kondering, U., Lindner, T., van Osch, M.J.P., Rohr, A., Jansen, O., Helle, M., 2015. Superselective pseudo-continuous arterial spin labeling angiography. Eur. J. Radiol. 84, 1758–1767. https://doi.org/10.1016/j.ejrad.2015.05.034

Kim, S.G., 1995. Quantification of relative cerebral blood flow change by flow-sensitive alternating inversion recovery (FAIR) technique: application to functional mapping. Magn. Reson. Med. 34, 293–301. https://doi.org/10.1002/mrm.1910340303

Lin, Z., Li, Y., Su, P., Mao, D., Wei, Z., Pillai, J.J., Moghekar, A., van Osch, M., Ge, Y., Lu, H., 2018. Non-contrast MR imaging of blood-brain barrier permeability to water. Magn. Reson. Med.

80, 1507–1520. https://doi.org/10.1002/mrm.27141
Lindner, T., Jansen, O., Helle, M., 2020. Ternary encoded super-selective arterial spin labeling for time-resolved flow territory mapping. Phys. Med. Biol. 65, 10NT01. https://doi.org/10.1088/1361-6560/ab7ef0
Lindner, T., Larsen, N., Jansen, O., Helle, M., 2017. Selective arterial spin labeling in conjunction with phase-contrast acquisition for the simultaneous visualization of morphology, flow direction, and velocity of individual arteries in the cerebrovascular system. Magn. Reson. Med. 78, 1469–1475. https://doi.org/10.1002/mrm.26542
Lu, H., Clingman, C., Golay, X., van Zijl, P.C.M., 2004. Determining the longitudinal relaxation time (T1) of blood at 3.0 Tesla. Magn. Reson. Med. 52, 679–682. https://doi.org/10.1002/mrm.20178
Lu, H., Ge, Y., 2008. Quantitative evaluation of oxygenation in venous vessels using T2-Relaxation-Under-Spin-Tagging MRI. Magn. Reson. Med. 60, 357–363. https://doi.org/10.1002/mrm.21627
Lu, H., Golay, X., Pekar, J.J., Van Zijl, P.C.M., 2003. Functional magnetic resonance imaging based on changes in vascular space occupancy. Magn. Reson. Med. 50, 263–274. https://doi.org/10.1002/mrm.10519
Luh, W.M., Wong, E.C., Bandettini, P.A., Hyde, J.S., 1999. QUIPSS II with thin-slice TI1 periodic saturation: a method for improving accuracy of quantitative perfusion imaging using pulsed arterial spin labeling. Magn. Reson. Med. 41, 1246–1254. https://doi.org/10.1002/(sici)1522-2594(199906)41:6<1246::aid-mrm22>3.0.co;2-n
Mora Álvarez, M.G., Stobbe, R.W., Beaulieu, C., 2019. High resolution continuous arterial spin labeling of human cerebral perfusion using a separate neck tagging RF coil. PloS One 14, e0215998. https://doi.org/10.1371/journal.pone.0215998
Nakamura, M., Yoneyama, M., Tabuchi, T., Takemura, A., Obara, M., Tatsuno, S., Sawano, S., 2013. Vessel-selective, non-contrast enhanced, time-resolved MR angiography with vessel-selective arterial spin labeling technique (CINEMA-SELECT) in intracranial arteries. Radiol. Phys. Technol. 6, 327–334. https://doi.org/10.1007/s12194-013-0204-7
Nery, F., Buchanan, C.E., Harteveld, A.A., Odudu, A., Bane, O., Cox, E.F., Derlin, K., Gach, H.M., Golay, X., Gutberlet, M., Laustsen, C., Ljimani, A., Madhuranthakam, A.J., Pedrosa, I., Prasad, P.V., Robson, P.M., Sharma, K., Sourbron, S., Taso, M., Thomas, D.L., Wang, D.J.J., Zhang, J.L., Alsop, D.C., Fain, S.B., Francis, S.T., Fernández-Seara, M.A., 2020. Consensus-based technical recommendations for clinical translation of renal ASL MRI. Magma N. Y. N 33, 141–161. https://doi.org/10.1007/s10334-019-00800-z
Obara, M., Togao, O., Beck, G.M., Shibukawa, S., Okuaki, T., Yoneyama, M., Nakamura, M., Honda, H., Van Cauteren, M., 2018. Non-contrast enhanced 4D intracranial MR angiography based on pseudo-continuous arterial spin labeling with the keyhole and view-sharing technique. Magn. Reson. Med. 80, 719–725. https://doi.org/10.1002/mrm.27074
Obara, M., Togao, O., Yoneyama, M., Okuaki, T., Shibukawa, S., Honda, H., Van Cauteren, M., 2017. Acceleration-selective arterial spin labeling for intracranial MR angiography with improved visualization of cortical arteries and suppression of cortical veins. Magn. Reson. Med. 77, 1996–2004. https://doi.org/10.1002/mrm.26275
Ohene, Y., Harrison, I.F., Nahavandi, P., Ismail, O., Bird, E.V., Ottersen, O.P., Nagelhus, E.A., Thomas, D.L., Lythgoe, M.F., Wells, J.A., 2019. Non-invasive MRI of brain clearance pathways using multiple echo time arterial spin labelling: an aquaporin-4 study. NeuroImage 188, 515–523. https://doi.org/10.1016/j.neuroimage.2018.12.026

Okell, T.W., 2019. Combined angiography and perfusion using radial imaging and arterial spin labeling. Magn. Reson. Med. 81, 182–194. https://doi.org/10.1002/mrm.27366

Okell, T.W., Chappell, M.A., Jezzard, P., 2013. A theoretical framework for quantifying blood volume flow rate from dynamic angiographic data and application to vessel-encoded arterial spin labeling MRI. Med. Image Anal. 17, 1025–1036. https://doi.org/10.1016/j.media.2013.06.005

Okell, T.W., Chappell, M.A., Woolrich, M.W., Günther, M., Feinberg, D.A., Jezzard, P., 2010. Vessel-encoded dynamic magnetic resonance angiography using arterial spin labeling. Magn. Reson. Med. 64, 698–706. https://doi.org/10.1002/mrm.22458

Petersen, E.T., Golay, X., 2007. Improved Inversion Efficiency in Arterial Spin Labeling Using Adiabatic Null Pulses. Proc ISMRM 1407.

Petersen, E.T., Lim, T., Golay, X., 2006. Model-free arterial spin labeling quantification approach for perfusion MRI. Magn. Reson. Med. 55, 219–232. https://doi.org/10.1002/mrm.20784

Qin, Q., Shin, T., Schär, M., Guo, H., Chen, H., Qiao, Y., 2016. Velocity-selective magnetization-prepared non-contrast-enhanced cerebral MR angiography at 3 Tesla: Improved immunity to B0/B1 inhomogeneity. Magn. Reson. Med. 75, 1232–1241. https://doi.org/10.1002/mrm.25764

Qin, Q., van Zijl, P.C.M., 2016. Velocity-selective-inversion prepared arterial spin labeling. Magn. Reson. Med. 76, 1136–1148. https://doi.org/10.1002/mrm.26010

Robson, P.M., Dai, W., Shankaranarayanan, A., Rofsky, N.M., Alsop, D.C., 2010. Time-resolved vessel-selective digital subtraction MR angiography of the cerebral vasculature with arterial spin labeling. Radiology 257, 507–515. https://doi.org/10.1148/radiol.092333

Schidlowski, M., Boland, M., Rüber, T., Stöcker, T., 2020. Blood-brain barrier permeability measurement by biexponentially modeling whole-brain arterial spin labeling data with multiple T2 -weightings. NMR Biomed. 33, e4374. https://doi.org/10.1002/nbm.4374

Schmid, S., Ghariq, E., Teeuwisse, W.M., Webb, A., van Osch, M.J.P., 2014. Acceleration-selective arterial spin labeling. Magn. Reson. Med. 71, 191–199. https://doi.org/10.1002/mrm.24650

Shao, X., Ma, S.J., Casey, M., D'Orazio, L., Ringman, J.M., Wang, D.J.J., 2019a. Mapping water exchange across the blood-brain barrier using 3D diffusion-prepared arterial spin labeled perfusion MRI. Magn. Reson. Med. 81, 3065–3079. https://doi.org/10.1002/mrm.27632

Shao, X., Zhao, Z., Russin, J., Amar, A., Sanossian, N., Wang, D.J., Yan, L., 2019b. Quantification of intracranial arterial blood flow using noncontrast enhanced 4D dynamic MR angiography. Magn. Reson. Med. 82, 449–459. https://doi.org/10.1002/mrm.27712

Shin, T., Hu, B.S., Nishimura, D.G., 2013. Off-resonance-robust velocity-selective magnetization preparation for non-contrast-enhanced peripheral MR angiography. Magn. Reson. Med. 70, 1229–1240. https://doi.org/10.1002/mrm.24561

Silva, A.C., Lee, S.P., Yang, G., Iadecola, C., Kim, S.G., 1999. Simultaneous blood oxygenation level-dependent and cerebral blood flow functional magnetic resonance imaging during forepaw stimulation in the rat. J. Cereb. Blood Flow Metab. Off. J. Int. Soc. Cereb. Blood Flow Metab. 19, 871–879. https://doi.org/10.1097/00004647-199908000-00006

Silva, A.C., Zhang, W., Williams, D.S., Koretsky, A.P., 1997. Estimation of water extraction fractions in rat brain using magnetic resonance measurement of perfusion with arterial spin labeling. Magn. Reson. Med. 37, 58–68. https://doi.org/10.1002/mrm.1910370110

Song, R., Loeffler, R.B., Hillenbrand, C.M., 2012. QUIPSS II with window-sliding saturation sequence (Q2WISE). Magn. Reson. Med. 67, 1127–1132. https://doi.org/10.1002/mrm.23093

St Lawrence, K.S., Lee, T.Y., 1998. An adiabatic approximation to the tissue homogeneity model for

water exchange in the brain: I. Theoretical derivation. J. Cereb. Blood Flow Metab. Off. J. Int. Soc. Cereb. Blood Flow Metab. 18, 1365–1377. https://doi.org/10.1097/00004647-199812000-00011

Su, P., Mao, D., Liu, P., Li, Y., Pinho, M.C., Welch, B.G., Lu, H., 2017. Multiparametric estimation of brain hemodynamics with MR fingerprinting ASL. Magn. Reson. Med. 78, 1812–1823. https://doi.org/10.1002/mrm.26587

Suzuki, Y., Fujima, N., Ogino, T., Meakin, J.A., Suwa, A., Sugimori, H., Van Cauteren, M., van Osch, M.J.P., 2018a. Acceleration of ASL-based time-resolved MR angiography by acquisition of control and labeled images in the same shot (ACTRESS). Magn. Reson. Med. 79, 224–233. https://doi.org/10.1002/mrm.26667

Suzuki, Y., Fujima, N., van Osch, M.J.P., 2020. Intracranial 3D and 4D MR Angiography Using Arterial Spin Labeling: Technical Considerations. Magn. Reson. Med. Sci. MRMS Off. J. Jpn. Soc. Magn. Reson. Med. 19, 294–309. https://doi.org/10.2463/mrms.rev.2019-0096

Suzuki, Y., Helle, M., Koken, P., Van Cauteren, M., van Osch, M.J.P., 2018b. Simultaneous acquisition of perfusion image and dynamic MR angiography using time-encoded pseudo-continuous ASL. Magn. Reson. Med. 79, 2676–2684. https://doi.org/10.1002/mrm.26926

Talagala, S.L., Ye, F.Q., Ledden, P.J., Chesnick, S., 2004. Whole-brain 3D perfusion MRI at 3.0 T using CASL with a separate labeling coil. Magn. Reson. Med. 52, 131–140. https://doi.org/10.1002/mrm.20124

Teeuwisse, W.M., Schmid, S., Ghariq, E., Veer, I.M., van Osch, M.J.P., 2014. Time-encoded pseudocontinuous arterial spin labeling: basic properties and timing strategies for human applications. Magn. Reson. Med. 72, 1712–1722. https://doi.org/10.1002/mrm.25083

van Osch, M.J.P., Hendrikse, J., Golay, X., Bakker, C.J.G., van der Grond, J., 2006. Non-invasive visualization of collateral blood flow patterns of the circle of Willis by dynamic MR angiography. Med. Image Anal. 10, 59–70. https://doi.org/10.1016/j.media.2005.04.010

von Samson-Himmelstjerna, F., Madai, V.I., Sobesky, J., Guenther, M., 2016. Walsh-ordered hadamard time-encoded pseudocontinuous ASL (WH pCASL). Magn. Reson. Med. 76, 1814–1824. https://doi.org/10.1002/mrm.26078

Wang, J., Alsop, D.C., Song, H.K., Maldjian, J.A., Tang, K., Salvucci, A.E., Detre, J.A., 2003. Arterial transit time imaging with flow encoding arterial spin tagging (FEAST). Magn. Reson. Med. 50, 599–607. https://doi.org/10.1002/mrm.10559

Wang, J., Fernández-Seara, M.A., Wang, S., St Lawrence, K.S., 2007. When perfusion meets diffusion: in vivo measurement of water permeability in human brain. J. Cereb. Blood Flow Metab. Off. J. Int. Soc. Cereb. Blood Flow Metab. 27, 839–849. https://doi.org/10.1038/sj.jcbfm.9600398

Wells, J.A., Lythgoe, M.F., Gadian, D.G., Ordidge, R.J., Thomas, D.L., 2010. In vivo Hadamard encoded continuous arterial spin labeling (H-CASL). Magn. Reson. Med. 63, 1111–1118. https://doi.org/10.1002/mrm.22266

Wells, J.A., Siow, B., Lythgoe, M.F., Thomas, D.L., 2013. Measuring biexponential transverse relaxation of the ASL signal at 9.4 T to estimate arterial oxygen saturation and the time of exchange of labeled blood water into cortical brain tissue. J. Cereb. Blood Flow Metab. Off. J. Int. Soc. Cereb. Blood Flow Metab. 33, 215–224. https://doi.org/10.1038/jcbfm.2012.156

Wengler, K., Bangiyev, L., Canli, T., Duong, T.Q., Schweitzer, M.E., He, X., 2019. 3D MRI of whole-brain water permeability with intrinsic diffusivity encoding of arterial labeled spin (IDEALS). NeuroImage 189, 401–414. https://doi.org/10.1016/j.neuroimage.2019.01.035

Werner, R., Alfke, K., Schaeffter, T., Nabavi, A., Mehdorn, H.M., Jansen, O., 2004. Brain perfusion

territory imaging applying oblique-plane arterial spin labeling with a standard send/receive head coil. Magn. Reson. Med. 52, 1443–1447. https://doi.org/10.1002/mrm.20253

Werner, R., Norris, D.G., Alfke, K., Mehdorn, H.M., Jansen, O., 2005. Continuous artery-selective spin labeling (CASSL). Magn. Reson. Med. 53, 1006–1012. https://doi.org/10.1002/mrm.20475

Williams, D.S., Detre, J.A., Leigh, J.S., Koretsky, A.P., 1992. Magnetic resonance imaging of perfusion using spin inversion of arterial water. Proc. Natl. Acad. Sci. 89, 212–216.

Wong, E.C., 2007. Vessel-encoded arterial spin-labeling using pseudocontinuous tagging. Magn. Reson. Med. 58, 1086–1091. https://doi.org/10.1002/mrm.21293

Wong, E.C., 2005. Quantifying CBF with pulsed ASL: Technical and pulse sequence factors. J. Magn. Reson. Imaging 22, 727–731. https://doi.org/10.1002/jmri.20459

Wong, E.C., Buxton, R.B., Frank, L.R., 1998a. Quantitative imaging of perfusion using a single subtraction (QUIPSS and QUIPSS II). Magn. Reson. Med. 39, 702–708. https://doi.org/10.1002/mrm.1910390506

Wong, E.C., Buxton, R.B., Frank, L.R., 1998b. A theoretical and experimental comparison of continuous and pulsed arterial spin labeling techniques for quantitative perfusion imaging. Magn. Reson. Med. 40, 348–355. https://doi.org/10.1002/mrm.1910400303

Wong, E.C., Buxton, R.B., Frank, L.R., 1997. Implementation of quantitative perfusion imaging techniques for functional brain mapping using pulsed arterial spin labeling. NMR Biomed. 10, 237–249. https://doi.org/10.1002/(sici)1099-1492(199706/08)10:4/5<237::aid-nbm475>3.0.co;2-x

Wong, E.C., Cronin, M., Wu, W.-C., Inglis, B., Frank, L.R., Liu, T.T., 2006. Velocity-selective arterial spin labeling. Magn. Reson. Med. 55, 1334–1341. https://doi.org/10.1002/mrm.20906

Yan, L., Li, C., Kilroy, E., Wehrli, F.W., Wang, D.J.J., 2012. Quantification of arterial cerebral blood volume using multiphase-balanced SSFP-based ASL. Magn. Reson. Med. 68, 130–139. https://doi.org/10.1002/mrm.23218

Yan, L., Wang, S., Zhuo, Y., Wolf, R.L., Stiefel, M.F., An, J., Ye, Y., Zhang, Q., Melhem, E.R., Wang, D.J.J., 2010. Unenhanced dynamic MR angiography: high spatial and temporal resolution by using true FISP-based spin tagging with alternating radiofrequency. Radiology 256, 270–279. https://doi.org/10.1148/radiol.10091543

Ye, F.Q., Frank, J.A., Weinberger, D.R., McLaughlin, A.C., 2000. Noise reduction in 3D perfusion imaging by attenuating the static signal in arterial spin tagging (ASSIST). Magn. Reson. Med. 44, 92–100. https://doi.org/10.1002/1522-2594(200007)44:1<92::aid-mrm14>3.0.co;2-m

Zhang, Q., Su, P., Chen, Z., Liao, Y., Chen, S., Guo, R., Qi, H., Li, X., Zhang, X., Hu, Z., Lu, H., Chen, H., 2020. Deep learning-based MR fingerprinting ASL ReconStruction (DeepMARS). Magn. Reson. Med. 84, 1024–1034. https://doi.org/10.1002/mrm.28166

Zhang, W., Silva, A.C., Williams, D.S., Koretsky, A.P., 1995. NMR measurement of perfusion using arterial spin labeling without saturation of macromolecular spins. Magn. Reson. Med. 33, 370–376. https://doi.org/10.1002/mrm.1910330310

Zhang, X., Petersen, E.T., Ghariq, E., De Vis, J.B., Webb, A.G., Teeuwisse, W.M., Hendrikse, J., van Osch, M.J.P., 2013. In vivo blood T(1) measurements at 1.5 T, 3 T, and 7 T. Magn. Reson. Med. 70, 1082–1086. https://doi.org/10.1002/mrm.24550

Zhao, J.M., Clingman, C.S., Närväinen, M.J., Kauppinen, R.A., van Zijl, P.C.M., 2007. Oxygenation and hematocrit dependence of transverse relaxation rates of blood at 3T. Magn. Reson. Med. 58, 592–597. https://doi.org/10.1002/mrm.21342